Journal of Hazardous Materials 194 (2011) 268–276

Contents lists available at ScienceDirect

Journal of Hazardous Materials

journal homepage: www.elsevier.com/locate/jhazmat

Stabilization of $ZnCl_2$-containing wastes using calcium sulfoaluminate cement: Leaching behaviour of the solidified waste form, mechanisms of zinc retention

Stéphane Berger[a], Céline Cau Dit Coumes[a,*], Jean-Baptiste Champenois[a], Thierry Douillard[b], Patrick Le Bescop[c], Georges Aouad[d,e], Denis Damidot[d,e]

[a] Commissariat à l'Energie Atomique et aux Energies Alternatives, CEA/DEN/MAR/DTCD/SPDE, BP17171, 30207 Bagnols-sur-Cèze cedex, France
[b] INSA-Lyon, MATEIS UMR5510, F-69621 Villeurbanne, France
[c] Commissariat à l'Energie Atomique et aux Energies Alternatives, CEA/DEN/SAC/DPC/SCCME, 91192 Gif/Yvette, France
[d] Univ. Lille Nord de France, 59000 Lille, France
[e] EM Douai, MPE-GCE, 59508 Douai, France

ARTICLE INFO

Article history:
Received 24 January 2011
Received in revised form 25 July 2011
Accepted 26 July 2011
Available online 5 August 2011

Keywords:
Waste management
Calcium sulfoaluminate cement
Zinc chloride
Leaching

ABSTRACT

To assess the potential of calcium sulfoaluminate cement to solidify and stabilize wastes containing high amounts of soluble zinc chloride (a strong inhibitor of Portland cement hydration), a simulated cemented waste form was submitted to leaching by pure water at a fixed pH of 7 for three months, according to a test designed to understand the degradation processes of cement pastes. Leaching was controlled by diffusion. The zinc concentration in the leachates always remained below the detection limit (2 μmol/L), showing the excellent confining properties of the cement matrix. At the end of the experiment, the solid sample exhibited three zones which were accurately characterized: (i) a highly porous and friable surface layer, (ii) a less porous intermediate zone in which several precipitation and dissolution fronts occurred, and (iii) the sound core. Ettringite was a good tracer for degradation. The good retention of zinc by the cement matrix was mainly attributed to the precipitation of a hydrated and well crystallized phase with platelet morphology (which may belong to the layered double hydroxide family) at early age (≤1 day), and to chemisorption onto aluminum hydroxide at later age.

© 2011 Elsevier B.V. All rights reserved.

1. Introduction

It has long been common practice to stabilize low-level radioactive wastes with cement. However, some waste components may react with cement phases, thus reducing the quality of the product.

For instance, ashes resulting from the incineration of technological wastes with neoprene and polyvinylchloride may contain substantial amounts of soluble zinc chloride [1]. This compound is known to have deleterious effects on hydration of Ordinary Portland cement (OPC). Setting is strongly delayed, and can even be inhibited at high zinc loadings [2,3], while hardening is slowed down [4–7]. Moreover, zinc in its ionic form is an environmental pollutant [8]. In humans, its prolonged and excessive intake (reference dose for chronic oral exposure of 0.3 mg/kg/day [9]) may lead to toxic effects, such as carcinogenesis, mutagenesis and teratogenesis, as a result of its accumulation [10].

One approach to limit adverse interactions is to select a binder showing a better compatibility with the waste. It has been recently shown that calcium sulfoaluminate (CSA) cements prepared from clinkers in which ye'elimite (or tetracalcium trialuminate sulfate, $C_4A_3\underline{S}$[1]) predominates over belite (C_2S) exhibit a much better compatibility with zinc chloride than OPC [11,12]: their setting is never inhibited, even at high concentration of $ZnCl_2$ (0.5 mol/L) in the mixing water, and zinc is readily insolubilized. The zinc concentration in the pore solution extracted from CSA cement pastes is already below the detection limit (2 μmol/L) of the analytical method (ICP-AES) after one day of hydration [12]. Blending the CSA clinker with 20% gypsum offers several advantages: (i) no hydration delay, contrarily to a gypsum-free binder, (ii) reduced temperature rise and cumulative heat produced during hydration, (iii) improved compressive strength of the hardened materials and limited expansion under wet curing, and (iv) mineralogy less dependent on a temperature rise and fall at early age, as may occur in a large-volume drum of cemented waste.

At 20 °C, the hydration progress of a CSA cement containing 20% gypsum and mixed with a 0.5 mol/L $ZnCl_2$ solution (water to cement ratio (w/c) = 0.55) occurs by the initial precipitation of amorphous aluminum hydroxide (AH_3), gypsum and an unidenti-

* Corresponding author. Tel.: +33 4 66 39 74 50; fax: +33 4 66 33 90 37.
E-mail address: celine.cau-dit-coumes@cea.fr (C. Cau Dit Coumes).

[1] Shorthand cement notations are used in this article: C = CaO, S = SiO_2, $\underline{S}$ = SO_3, A = Al_2O_3, H = H_2O, T = TiO_2.

0304-3894/$ – see front matter © 2011 Elsevier B.V. All rights reserved.
doi:10.1016/j.jhazmat.2011.07.102

Table 1
Mineralogical composition of the investigated CSA clinker (KTS 100 provided by Belitex).

Minerals	$C_4A_3\underline{S}$	C_2S	$C_{12}A_7$	CT	Periclase	$C\underline{S}$	Quartz	Others[a]
Wt%	68.5	15.9	9.5	2.9	1.5	0.5	0.5	2.4

[a] Include 1.2% of iron oxide.

fied compound, referred to as "phase λ", which exhibits a platelet morphoplogy. Ettringite then precipitates while gypsum is rapidly depleted. Phase λ is fully consumed beyond one day of hydration. From 7 d to 360 d, the phase assemblage evolves very slowly and comprises ettringite, AH_3, and small amounts of Friedel's salt, an AFm phase in which the positively charged main layers are balanced by the insertion of chloride anions in the interlayer ($C_3A{\cdot}CaCl_2{\cdot}10H_2O$). Fully hydrated materials contain ettringite, AH_3, strätlingite (C_2ASH_8), Friedel's salt and Kuzel's salt, another AFm-structured compound containing ordered chloride and sulfate anions ($C_3A{\cdot}1/2CaSO_4{\cdot}1/2CaCl_2{\cdot}10H_2O$) in its interlayer. From 1 d and the depletion of phase λ, crystallized zinc-containing phases can no longer be detected in the material. However, zinc is very efficiently insolubilized, as shown by analyses of the pore solution extracted from cement pastes at various ages, and of the curing solution of mortars kept one year under water: the zinc concentration is always below the detection limit (2 μmol/L) [12].

This work complements our previous study and aims at elucidating the mechanisms of zinc retention by a CSA cement paste. In this purpose, a CSA cement paste containing zinc chloride was submitted to leaching by pure water according to a test developed by the CEA [13] in order to understand the degradation processes of the cement hydrates. Unlike previous work mainly focussed on the analysis of the leachates [14], particular attention was also brought to the mineralogical evolutions caused by the leaching process in the cement matrix.

2. Experimental

2.1. Materials and specimen preparation

CSA cements were prepared by mixing a ground industrial CSA clinker (the composition of which is summarized in Table 1; d_{10} = 2.67 μm, d_{50} = 17.6 μm, d_{90} = 50.8 μm, BET specific surface area = 1.3 m^2/g) with 20% (by weight of cement) of analytical grade gypsum (d_{10} = 5.4 μm, d_{50} = 19.6 μm, d_{90} = 50.3 μm, BET specific surface area = 0.4 m^2/g) for 15 min. In the clinker, ye'elimite predominated over belite and mayenite. The other minor constituents, mainly phases containing titanium and iron, could be regarded as hydraulically inactive. A cement paste (w/c of 0.55) was prepared with a standardized laboratory mixer (following European standard EN 196-1) by mixing cement and a solution of zinc chloride (concentration of 0.5 mol/L) at low speed for 3 min, and at high speed for 2 min. The $ZnCl_2$ solution was obtained by dissolving the appropriate amount of analytical grade salt in distilled water. The 0.5 mol/L concentration was representative of the concentration released in the mixing water by actual radioactive incinerator ashes. The paste was then cast into airtight polypropylene boxes, submitted to a brief thermal excursion at early age in an oven (Memmert UFP 500), as may occur in a 200-L drum filled with cemented waste, and subsequently cured for three months at 95% relative humidity and 20 °C. The thermal cycle was previously described in [12] (sample Z2t): the maximum temperature (79 °C) was reached 5 h after mixing, the sample was maintained over 70 °C for 9 h, and the cooling to ambient temperature took 6 days. Application of the thermal treatment was justified by previous results showing that the physico-chemical evolution of CSA cement-based materials can be dependent on their thermal history at early age [15].

2.2. Leaching test

After 3 months of curing (20 °C, 95% R.H), two cylinders (5 cm in diameter, 3 cm high, protected against lateral degradation by a polymer coating) of the cement paste were leached in deionized and decarbonated water thermo-regulated at 20 ± 1 °C, and kept under N_2 atmosphere to avoid carbonation. A sketch of the device is given in Fig. 1. The ratio between the sample surface area and the solution volume was fixed to 0.46 dm^2/L. This ratio represented a good compromise between the frequency of the leaching solution renewals, and the level of concentrations to be measured in the leachates. The composition of the leaching solution remained constant during the test, with a pH maintained at 7.0 by adding nitric acid (0.25 mol/L) in the reactor. The leaching solution was renewed when the volume of added nitric acid reached 1% of the solution volume. After each renewal, the solution was sampled and analysed by ionic chromatography (SO_4^{2-} and Cl^- concentrations determined with an accuracy of ±5%) and ICP-AES (Ca, Al, Si and Zn concentrations, measured with an accuracy of ±3%). The mineralogy of the leached zone was assessed by progressively scraping the samples from the external surface to the sound core using a micromilling machine. With the help of XRD, TGA, and SEM/EDX, it was possible by this way to determine the phases within slices approximately 100 μm thick, parallel to the leached surface.

2.3. Characterization methods

Crystallized phases were identified by X-ray diffraction (Siemens D8 – Copper anode $\lambda_{K\alpha1}$ = 1.54056 Å generated at 40 mA and 40 kV) on pastes ground to a particle size of less than 100 μm. The acquisition range was from 5° to 60° 2θ at 0.02° 2θ steps with integration at the rate of 50 s per step. Thermogravimetric analyses were carried out under N_2 atmosphere on 50 ± 2 mg of sample

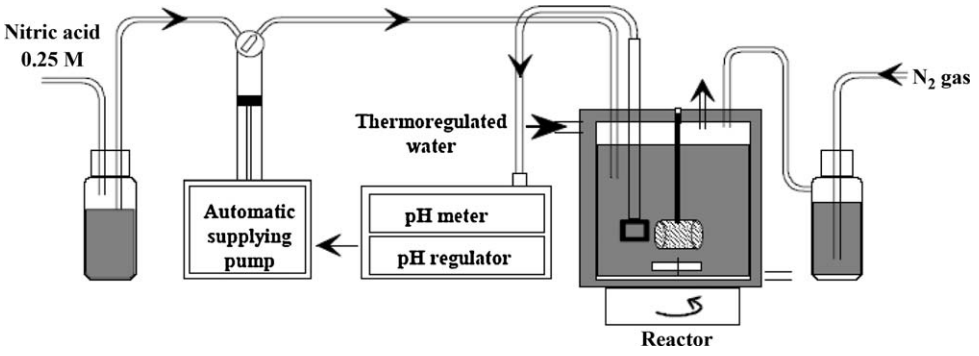

Fig. 1. Leaching device.

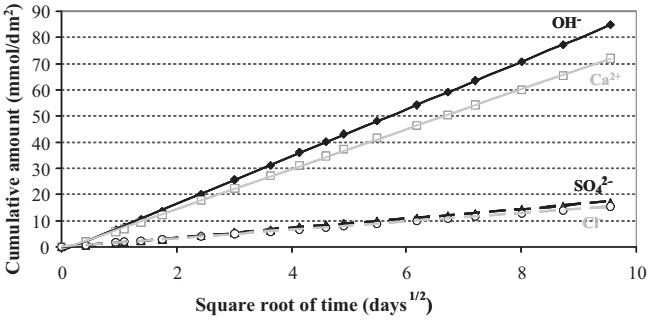

Fig. 2. Cumulative amounts of Ca^{2+}, SO_4^{2-}, Cl^- and OH^- ions released during leaching of the cement paste in deionized water (pH 7, 20 °C).

using a TGA/DSC Netzsch STA 409 PC instrument at 10 °C/min up to 1000 °C.

The microstructure and chemical composition of the cement pastes was investigated using SEM (JEOL JSM-5910 LV with a tungsten filament, or ESEM XL30-FEI microscope equipped with a thermal field emission gun). X-ray microanalyses were performed using an energy dispersive X-ray system (EDX EDAX type). In the STEM-in-SEM mode (FEI ESEM XL-30), a 3 mm diameter TEM copper grid with the sample was placed on the head of a TEM sample holder fixed on a vertical axis set to the stage of the SEM. The incident electron beam passed through the sample. The signal was then collected by an annular semi-conductor detector, classically used for the collection of backscattered electrons. In our experiments, the detector was located below the sample and enabled to collect electrons that were scattered by the sample, transmitted electrons passing through the hole located at the center of the STEM detector. Using this method, a large fraction of the scattered electrons was available to form an image and high contrast dark field images could be obtained.

Additional observations were performed with a 200 kV field emission gun transmission electron microscope (JEOL 2010F) equipped with an energy dispersive spectrometry system (INCA-OXFORD EDX) with a detector dedicated to light element detection.

All samples observed by STEM-in-SEM or TEM were prepared using the following procedure: some hydrated cement particles were scrapped from the specimen using a scalpel. Then, they were dispersed in methanol using an ultrasonic bath. Several dilutions were performed to obtain a very low material concentration. A drop of suspension was then laid down on a 200 mesh copper grid, covered on the back with a holey carbon film. The excess of methanol was soaked away using filter paper.

3. Results

3.1. Characterization of the leachates

Fig. 2 presents the cumulative quantities of OH^-, Ca^{2+}, SO_4^{2-} and Cl^- released in the leaching solution as a function of the square root of time. They increased linearly, showing that leaching was controlled by diffusion. The corresponding fluxes were respectively 9.03 ± 0.04 mmol/dm^2/day$^{0.5}$ (OH^-), 7.63 ± 0.03 mmol/dm^2/day$^{0.5}$ (Ca^{2+}), 1.82 ± 0.01 mmol/dm^2/day$^{0.5}$ (SO_4^{2-}), and 1.59 ± 0.01 mmol/dm^2/day$^{0.5}$ (Cl^-). Silicates and aluminates were not detected in the solution. However, an amorphous white compound, identified as aluminum hydroxide by EDX microanalysis, precipitated in the leachates. The zinc concentration always remained below the detection limit of the ICP method (2 μmol/L), meaning that, for the whole test (18 renewals), the leached fraction of zinc was less than 0.1%. The cement matrix thus provided good confinement of zinc.

3.2. Characterization of the degraded solid

We tried to estimate the position of the degradation front in the cement paste after 3 months of leaching. For OPC-based materials, such a period of leaching is long enough to get a significant depth of degradation, and the dissolution of portlandite is a good indicator for the location of the degradation front [13]. However, the tracer for the degradation of CSA-based materials was unknown. Different techniques were thus combined: SEM observations and X-ray microanalysis, as well as X-ray diffraction.

The first approach was to use chemical contrast from SEM/BSE images, the density of the degraded zone being lower than that of the sound core due to decalcification. A sharp transition was effectively observed between a bright zone (sound core) and a dark one (degraded material) (Fig. 3). The degradation depth was around 700 μm. Ca- and S-mapping clearly showed the decalcification and sulfur loss from the cement paste near the surface exposed to leaching, in a zone with a thickness of 700 μm, which was in good agreement with the estimation derived from the BSE image. The silicate density in this zone appeared to increase slightly. The Cl-mapping revealed however that chlorides were leached within a larger domain, up to a depth of 1600 μm from the surface. The alumina and zinc content appeared to remain relatively constant whatever the considered depth.

In a second approach, XRD analyses were carried out on the samples surface which was scrapped off step by step (thickness ≈ 100 μm for each step) to obtain XRD profiles (Fig. 4). The first signs of alteration were noticed from a depth of 2500 μm. Several processes were observed:

- dissolution of the Friedel's salt (from 2500 μm to 1900 μm) and of the Kuzel's salt (from 1900 to 1500 μm) which released chlorides,
- transient precipitation of monosulfoaluminate (from 2100 to 1300 μm),
- dissolution of monosulfoaluminate (from 1500 to 1300 μm) and of residual ye'elimite (from 1300 to 1100 μm),
- dissolution of ettringite (from 1500 to 700 μm).

The surface layer, with a depth of 700 μm (consistent with the SEM observations), was mainly composed of perovskite, of poorly crystallized aluminum hydroxide which was clearly evidenced by TGA thanks to its water loss at 262 °C (Fig. 5c), and probably of C–A–S–H. These latter were not identified with certainty, but the leached silicate flux was below the detection limit and STEM analyses performed on the surface layer showed the presence of small amounts of calcium and silicon, together with aluminum (Fig. 5a and b). In addition, TGA curves exhibited a weight loss at 98 °C which could correspond to C–A–S–H (Fig. 5c). This surface layer was highly porous and friable.

To summarize, examination of the cement paste after three months revealed three zones:

- the surface layer, with very low mechanical strength, composed of aluminum hydroxide, perovskite and C–A–S–H, which could be easily detected from BSE images, Ca- and S-mapping (EDX analysis), and X-ray diffraction (disappearance of the ettringite signal),
- a less porous intermediate zone, in which several precipitation and dissolution fronts occurred, as shown by X-ray diffraction and Cl-mapping (EDX analysis),
- the sound core.

Zinc was homogeneously distributed in all the three zones, which rules out the assumption of dissolution in the intermediate zone, followed by reprecipitation in the surface layer.

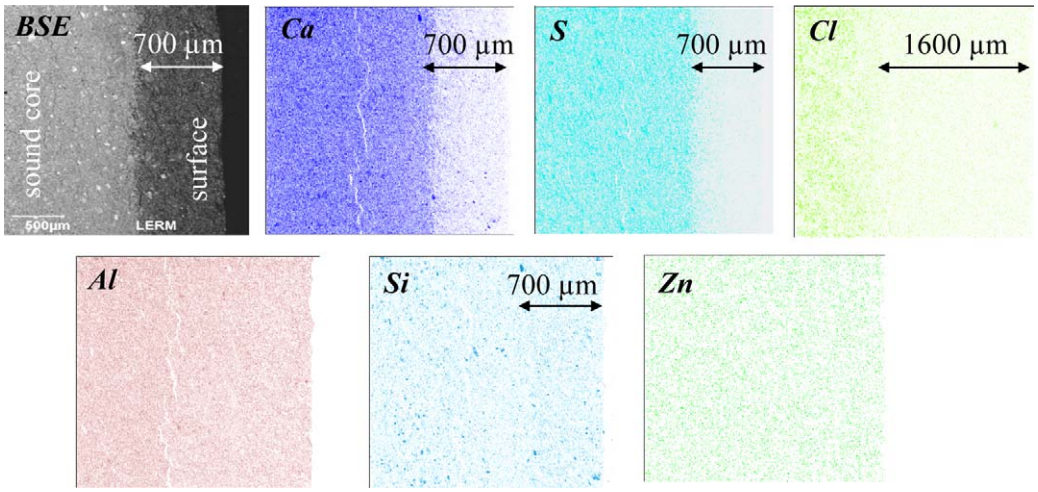

Fig. 3. SEM characterization of the cement paste after 3 months of leaching (pure water, pH 7, 20 °C): BSE picture and elemental mapping.

4. Discussion

Zinc was efficiently immobilized by the CSA cement matrix, as shown by the leaching test performed on the cement paste. This raised the question of its speciation in the solid phase.

4.1. Zinc speciation in the CSA matrix at early age

As mentioned in Section 1, in the cement pastes prepared with a $ZnCl_2$ solution, transient precipitation of phase λ was observed during the first hours of hydration, and was responsible for a rapid stiffening of the grout [11,12]. This phase was no longer detected in the absence of zinc (cement mixed with pure water, or with a $CaCl_2$ solution – Fig. 6a). Moreover, its formation was promoted by the addition of gypsum to the binder and strongly limited the precipitation of aluminum hydroxide at early age, as compared to reference materials prepared with pure water [12]. These results suggest that phase λ may contain zinc, aluminum and possibly sulfates. It was characterized by two X-ray diffraction peaks at $d_1 = 11.26$ Å (main intensity) and $d_2 \approx d_1/2 = 5.64$ Å. It also exhibited water loss around 95 °C, and possibly 195 °C, indicating that it was a hydrated phase. SEM observations of the CSA cement paste just after stiffen-

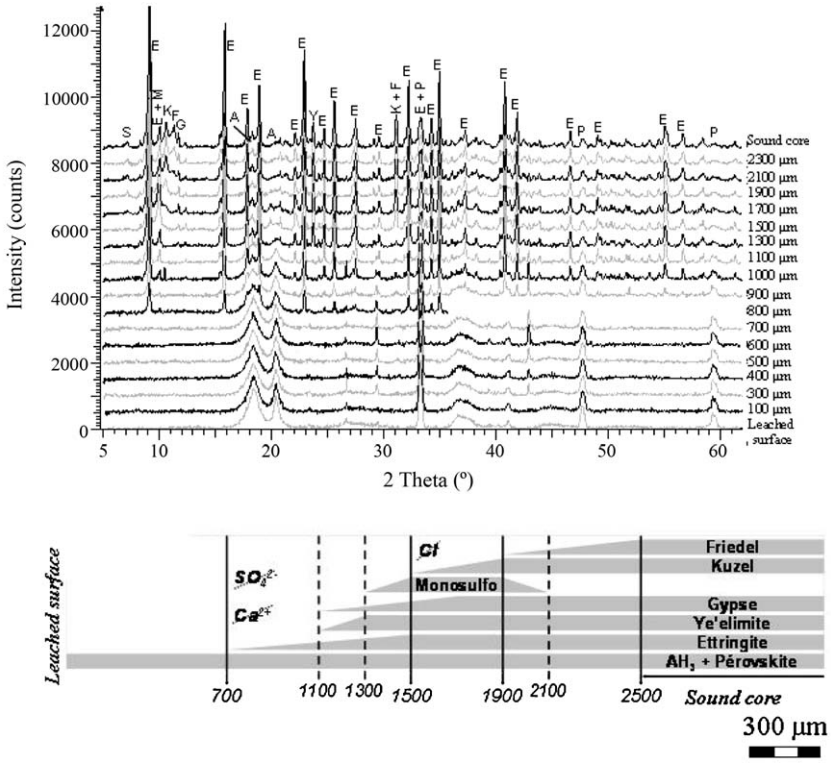

S= strätlingite, E = ettringite, M = monosulfoaluminate, K = Kuzel's salt, F = Friedel's salt; G = gypsum, A = aluminum hydroxide, Y = ye'elimite, P = perovskite

Fig. 4. XRD pattern of the degraded zone of the cement paste (from the surface (bottom) to the sound core (top)) after 3 months of leaching (pure water, pH 7, 20 °C).

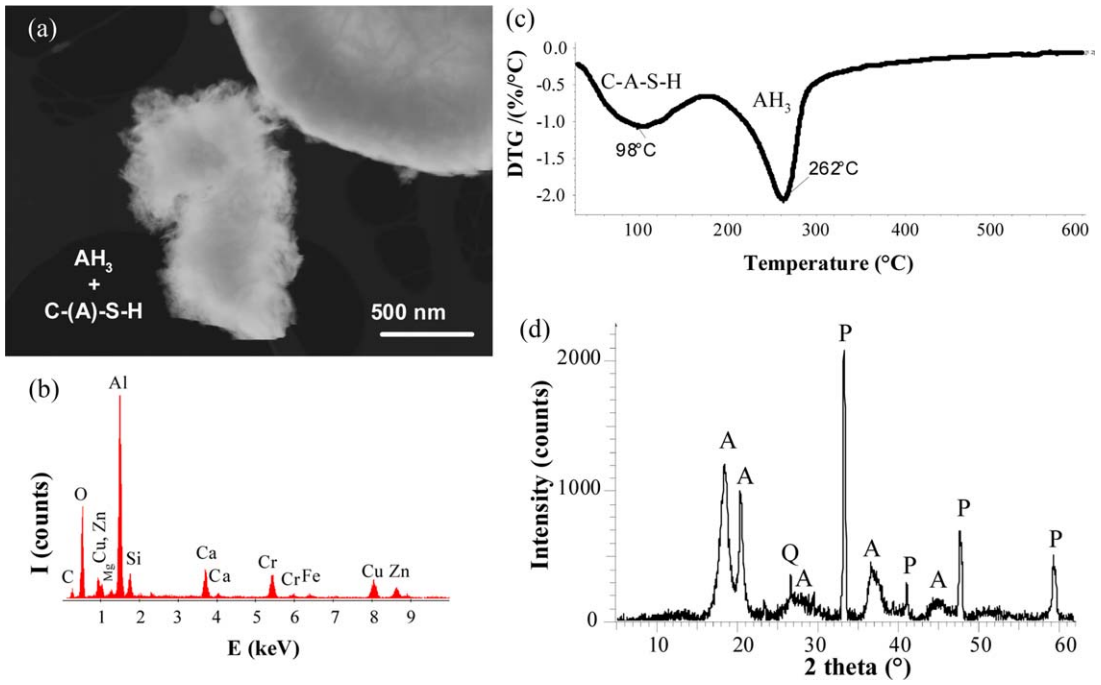

Fig. 5. Characterization of the leached surface of the cement paste: (a) particle observed in STEM-in-SEM (secondary electron image), (b) corresponding EDX analysis (carbon comes from the sample holder, Cu from the copper grid, and Cr from the detector), (c) TGA analysis of 50 mg of powder scraped from the surface, (d) XRD pattern (A: gibbsite, P: perovskite, Q: quartz).

ing showed the precipitation of hexagonal platelets at the surface of the clinker grains (Fig. 6b, and [12]). The crystals were too fine to be accurately analysed by EDX. Their morphology is typical of layered double hydroxides (LDH). [Zn–Al–Cl] LDHs or Zn/Al hydrotalcite ($Zn_6Al_2(OH)_{16}CO_3{\cdot}4H_2O$) were excluded because of their very different diffraction patterns [16–18]. A possible candidate might be zinc aluminum sulfate hydrate $5ZnO{\cdot}Al_2O_3{\cdot}ZnSO_4{\cdot}15H_2O$, which, according to JCPDS file number 44-0600, has a hexagonal lattice, and gives by X-ray diffraction a strong line at $d = 11.13$ Å (diffraction plane (0, 0, 6)), and two less intense lines at $d = 5.57$ Å (diffraction plane (0, 0, 12)) and $d = 3.72$ Å (diffraction plane (12, 0, 0)). We synthesized this compound according to the protocol of Pollmann and Vogel [19] by dissolving aluminum in 1 mol/L NaOH, and mixing it with aqueous $ZnSO_4{\cdot}7H_2O$ in stoichiometric ratio with excess water at 25 °C. Precipitation occurred almost instantaneously. The solid crystallized as small hexagonal platelets and exhibited the expected diffraction pattern (strong line at $d = 11.13$ Å, and two secondary lines at $d = 5.59$ Å and $d = 3.72$ Å). Three weight losses were recorded by thermogravimetry at 79 °C (main variation), and 176 and 277 °C. These characteristics differed slightly from those of phase λ, and it could not be concluded with certainty that phase λ was a zinc aluminum sulfate hydrate.

4.2. Zinc speciation in the CSA matrix at later age

Although zinc was efficiently insolubilized, crystallized Zn-containing phases could not be detected beyond one day. Several uptake mechanisms could be considered, including, incorporation in mineral structures through coprecipitation or lattice diffusion, precipitation, and adsorption on mineral surfaces.

4.2.1. Incorporation in the structure of AFm or AFt phases

The Zn^{2+}/Ca^{2+} substitution in the structure of ettringite is often postulated to account for the good retention of zinc by cement

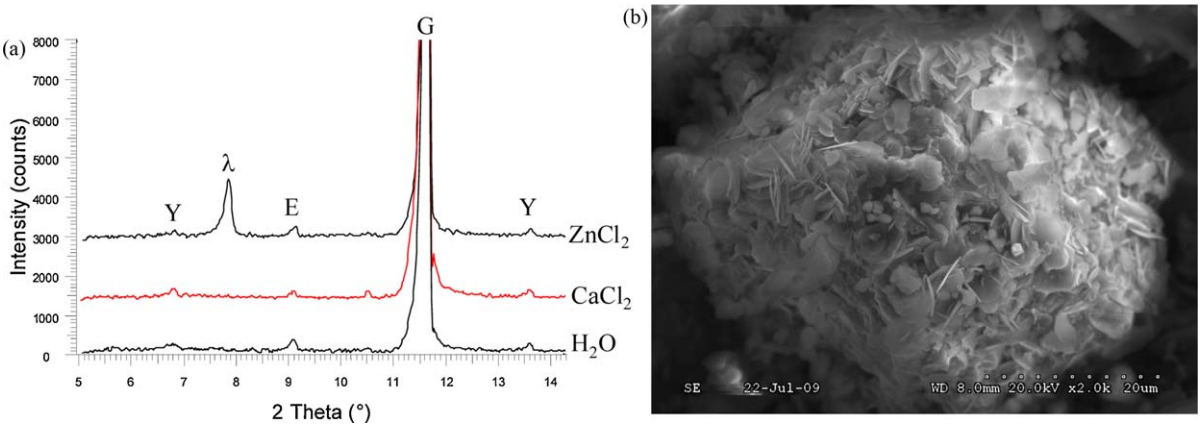

Fig. 6. Precipitation of phase λ at early age in $ZnCl_2$-rich samples. (a) Comparison of the XRD patterns recorded on cement pastes (80% CSA clinker + 20% gypsum) prepared with pure water, $CaCl_2$ (0.5 mol/L), or $ZnCl_2$ (0.5 mol/L) solution 1 h after mixing (Y: ye'elimite, G: gypsum, λ: phase λ). (b) SEM observation of phase λ over a clinker grain a few minutes after mixing.

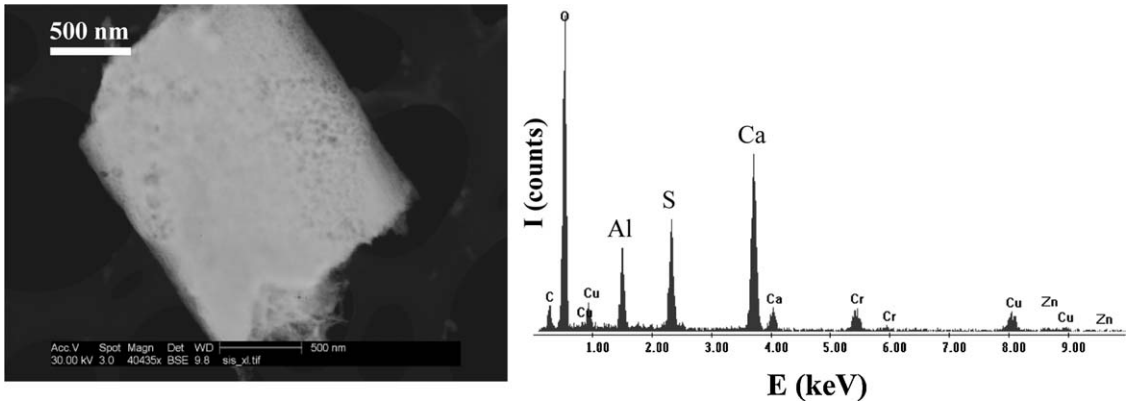

Fig. 7. STEM-in-SEM/EDX microanalysis of ettringite (carbon comes from the sample holder, Cu from the copper grid, and Cr from the detector).

pastes containing this hydrate [14,20–25]. However, some of our experimental results contradict this assumption.

(i) Some particles of hydrated cement were observed using the STEM-in-SEM (scanning transmission electron microscopy in the scanning electron microscope) technique and analysed by EDX. The much lower electron energy (30 kV) in the STEM-in-SEM versus TEM presented two main advantages for this study. First, the degradation of fragile phases such as ettringite under the electron beam [26] was limited. Second, the contrast enhancement was improved, which limited the excited volume and increased the electron scattering cross-section. Numerous particles of ettringite from the cement paste were characterized (Fig. 7), but none of them contained zinc. Similar results were obtained for AFm phases.

(ii) Elemental mapping was performed using SEM/EDX on a polished section of the sound core of the cement paste. Zinc was absent from the zones rich in sulfur (ettringite and calcium monosulfoaluminate) or chloride (Kuzel's or Friedel's salt) (Fig. 8).

(iii) We tried to synthesize ettringite with partial (molar ratio Zn/(Zn + Ca) of 0.1 or 0.75) or total substitution of Ca^{2+} ions by Zn^{2+} ions. Two methods are commonly used to synthesize pure ettringite. The classical method [27] consists in mixing calcium oxide and aluminum sulfate or gypsum and tricalcium aluminate in stoichiometric ratio with excess water, and stirring the suspension for several weeks, before filtering. In the saccharose method [28], precipitation of ettringite is strongly accelerated. Calcium oxide is first dissolved in a solution containing 10% (by weight) of saccharose. Aluminum sulfate is then added and ettringite forms almost instantaneously. Both methods were tested in this study. In the syntheses aiming at a total substitution of calcium by zinc, calcium oxide was replaced by $ZnSO_4$, ZnO, $ZnCl_2$ or $Zn(NO_3)_2$.

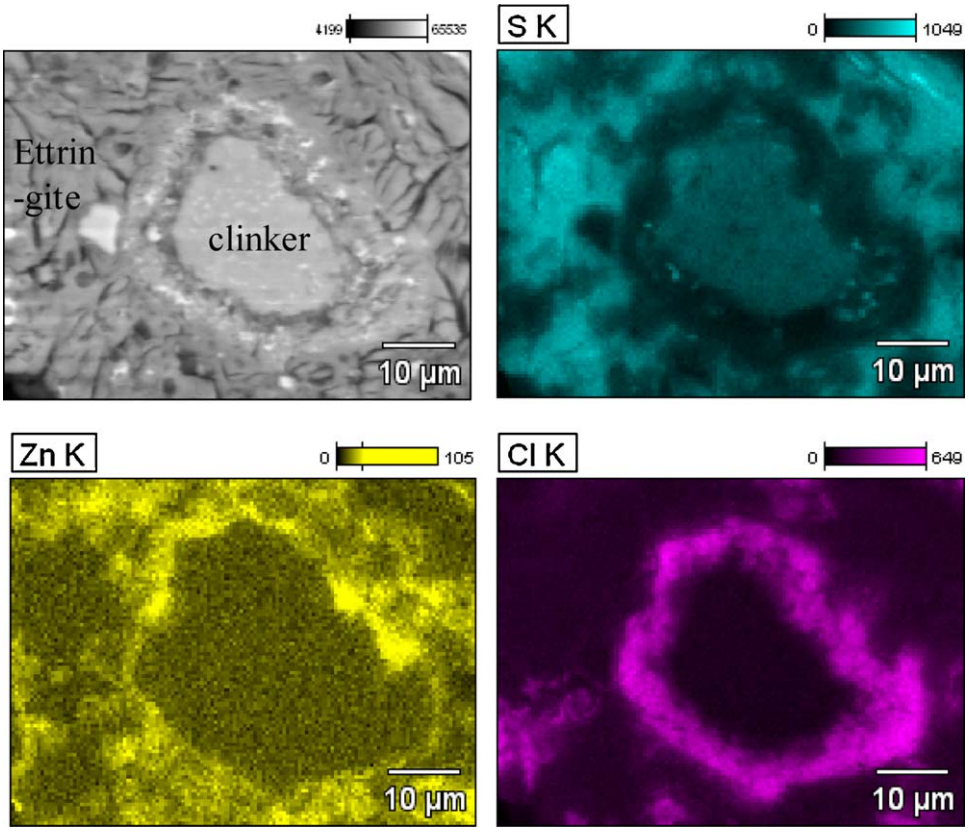

Fig. 8. SEM observation of a polished section of the sound cement paste (6-month old): BSE image, S, Zn and Cl-mappings using EDX analysis.

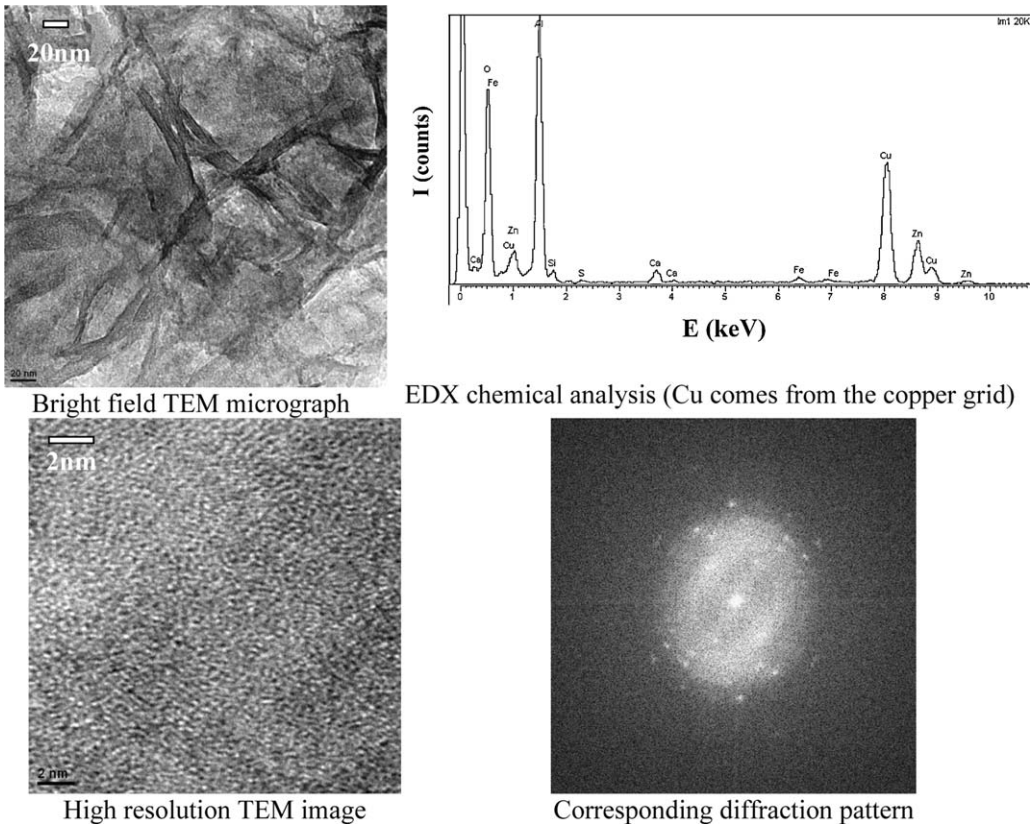

Fig. 9. TEM characterization of a particle from the surface layer of the cement paste after 3 months of leaching (pure water, pH 7, 20 °C).

To obtain only partial substitution, zinc sulfate was substituted for calcium oxide with Zn/(Zn + Ca) molar ratios of 0.1 or 0.75. In this case, sulfate exceeded the stoichiometry of ettringite. The pH was adjusted between 10 and 12 by adding sodium hydroxide. All the experiments were performed at 25 °C under nitrogen atmosphere with decarbonated water and lasted from 1 min to 6 weeks. When calcium was totally substituted by zinc, precipitation of an AFt phase did not occur. Zinc was insolubilized as zinc oxide (ZnO), zinc hydroxide ($Zn(OH)_2$), zinc sulfate hydrate ($[Zn(OH)_2]_3{\cdot}ZnSO_4{\cdot}3H_2O$ or $[Zn(OH)_2]_3{\cdot}ZnSO_4{\cdot}5H_2O$), and/or zinc aluminum sulfate hydrate ($5ZnO{\cdot}Al_2O_3{\cdot}ZnSO_4{\cdot}15H_2O$). When calcium was partly substituted by zinc, ettringite was precipitated with zinc aluminum sulfate hydrate ($5ZnO{\cdot}Al_2O_3{\cdot}ZnSO_4{\cdot}15H_2O$) and/or calcium zincate ($Zn_2Ca(OH)_6{\cdot}2H_2O$). The ettringite crystals were free of zinc, as shown by SEM/EDX analyses and by their diffraction pattern which corresponded perfectly with that of pure ettringite.

4.2.2. *Precipitation as an amorphous compound or as nanocrystals undetectable by X-ray diffraction*

Precipitation of zinc hydroxide or calcium zincate has already been reported in a Portland cement paste [29–33]. Other phases should also be considered in our systems.

- Simonkolleite $Zn_5(OH)_8Cl_2$ has been observed in zinc rusts formed under marine atmosphere [34] and is stable in slightly alkaline medium. It was transiently detected by X-ray diffraction instead of phase λ at early age in a cement paste (20% gypsum) prepared with a 2 mol/L $ZnCl_2$ solution. Its TGA diagram showed significant weight loss around 500 °C. Such a variation was however never observed in the pastes prepared with a 0.5 mol/L $ZnCl_2$ solution. Precipitation of simonkolleite in those materials thus seemed rather unlikely.
- Basic zinc sulfates $ZnSO_4{\cdot}Zn(OH)_2{\cdot}nH_2O$ have been identified during the cementation process of lead metal from lead sulfate slurries, zinc being used as the precipitant [35]. Such compounds also formed during the attempted syntheses of Zn-AFt phases.
- LDHs consist in a stacking of positively charged octahedral sheets with $[M^{II}_{1-x}M^{III}_x(OH)_2]^{x+}$ composition. They can be prepared with Zn^{2+} and Al^{3+} as the divalent M^{II} and trivalent M^{III} metal ions [36]. The net positive charge, due to substitution of divalent by trivalent metal ions, is balanced by an equal negative charge of the interlayer solvated anions $[X_{x/m}{}^{m-}{\cdot}nH_2O]^{x-}$. [Zn–Al–Cl] LDHs have been synthesized by coprecipitation in aqueous solution with a pH ideally comprised between 9 and 12, ZnO becoming predominant at higher pH [16,17]. These compounds seem however to be unstable in the presence of sulfates: their layered structure is damaged by ion exchange with $SO_4{}^{2-}$ and precipitation of basic zinc sulfates is observed [18].

The relatively low zinc content (1.2 weight % Zn) of the cement paste and its large number of phases made the detection of zinc precipitates difficult. However, after 3 months of leaching by pure water, this sample exhibited a simplified mineralogy in its degraded zone which still contained zinc, as shown by EDX elemental mapping (Fig. 5). Particular attention was thus paid to the surface layer. None of its X-ray diffraction peaks or weight losses by TGA could be ascribed to one of the above-mentioned zinc species. In particular, the absence of any weight loss at 155 °C or 290 °C excluded the occurrence of zinc hydroxide [37] or basic zinc sulfates [35].

Zinc did not precipitate as a crystalline phase and its occurrence as a specific amorphous or nanocrystalline product did not seem very likely.

4.2.3. Adsorption on mineral surfaces

The hypothesis of zinc adsorption on anhydrous cement phases can be ruled out for the following reasons. (i) Most of them were rapidly consumed in the cement paste. (ii) Perovskite was unreactive, but elemental mapping using EDX analysis did not show any concentration of zinc in the titanium-rich zones. Particular attention was paid to the surface layer, which still contained perovskite, but which exhibited a simpler mineralogy than the sound core. Even under these conditions favourable to observation, zinc was not associated with titanium, making the assumption of zinc sorption onto perovskite very unlikely.

Sorption of zinc onto C–S–H has already been described at low zinc concentrations [38]. The most probable mechanism is an incorporation of Zn(II) in the interlayer of C–S–H [39,40], rather than an exchange for Ca^{2+} [41]. Precipitation of C–S–H in the sound paste was not clearly evidenced, the Si-bearing phase being rather strätlingite. However, the formation of C–A–S–H was suspected in the degraded materials after leaching. EDX analyses performed on the surface layer showed the simultaneous presence of Ca, Al, Si and Zn (Fig. 5). If we assume a complete hydration of belite into C–S–H with a Ca/Si ratio of 2/3, and if we suppose, as shown by Stumm et al. [42], that the maximum zinc incorporation rate in such hydrates is 1/6, the fraction of zinc sorbed onto C–S–H in the cement paste could not exceed 36%, which is insufficient to explain the excellent retention of zinc by these materials.

The other candidate for zinc sorption is aluminum hydroxide which is formed in significant amounts by hydration of CSA cement. The most likely form is poorly crystallized gibbsite, as shown by the XRD pattern recorded on the surface layer of the leached sample (Fig. 5d). Sorption of zinc onto metal oxyhydroxides has been thoroughly investigated since the process is of importance to understand the migration of potentially toxic metal ions in soil and sediments environments [43]. According to Pokrovsky et al. [44], the threshold pH for zinc adsorption on gibbsite is about 6, and adsorption increases abruptly above this pH. Moreover, Chlorides promote the sorption of chloro-complexes (such as $ZnCl^+$), while sulfates enhance the cationic adsorption by making the surface potential more negative, as shown by Micera et al. [45] for amorphous aluminum hydroxide. Extended X-ray absorption fine structure spectroscopy has been used to probe the Zn atomic environment at the metal/gibbsite interface, showing that at low sorption densities, Zn(II) forms predominantly inner-sphere bidentate surface complexes with AlO_6 polyhedra, whereas at higher sorption densities the formation of a mixed-metal Zn(II)–Al(III) coprecipitate occurs with a layered double hydroxide structure [46,47].

STEM-in-SEM and TEM were used to characterize cement particles from the sound core and leached surface of the cement paste. X-ray microanalyses confirmed that zinc was always associated with a significant amount of aluminum attributed to aluminum hydroxide. In TEM, it was shown that the Zn-rich zones exhibited poor crystallinity (Fig. 9). LDHs phases being well crystallized, their presence seemed unlikely. Moreover, the aluminum hydroxide content (around 30 molar%) was much higher than that of zinc (less than 1 molar%) in hydrated cement pastes, which suggested a low Zn(II) sorption density and a sorption mechanism involving the binding of Zn(II) to AlO_6 in an edge-sharing bidentate geometry. Besides, a parallel may be drawn between the precipitation of phase λ occurring in our materials at early age, when the zinc/hydrates ratio is high, and the situation described by Trainor et al. [46] at high Zn(II) sorption densities, leading to the dissolution of the aluminum substrate and the reprecipitation of a mixed Zn-Al hydroxide coprecipitate with LDH structure.

5. Conclusion

The main conclusions of this work can be summarized as follows.

1. A simulated cemented waste form (cement paste prepared with a binder containing 20% gypsum and a 0.5 mol/L $ZnCl_2$ mixing solution, and submitted to a thermal cycle at early age) was submitted to leaching by pure water (fixed pH of 7) for three months. The cumulative quantities of Ca^{2+}, OH^-, Cl^- and SO_4^{2-} ions in the leachates increased linearly versus the square root of time, showing that leaching was controlled by diffusion. Zinc was never detected, showing the excellent confining properties of the cement matrix. Examination of the solid sample at the end of the experiment revealed three zones: (i) the surface layer, highly porous and friable, composed of aluminum hydroxide, perovskite and probably C–(A)–S–H (thickness: 700 μm), (ii) an intermediate zone, less porous, in which several precipitation and dissolution fronts occurred (thickness: 1800 μm), and (iii) the sound core. Ettringite was a good tracer for the degradation of CSA-cement based materials submitted to leaching by pure water.
2. The confinement of zinc by the cement matrix was attributed at early age (<1 day) to the precipitation of phase λ, a hydrated and well crystallized compound with platelet morphology, possibly a layered double hydroxide, the stoichiometry of which remains unidentified. At later age, the most probable mechanism was sorption of Zn^{2+} onto aluminum hydroxide (which involved the binding of Zn^{2+} to AlO_6 in an edge-sharing bidentate geometry), rather than a $Zn^{2+} \leftrightarrow Ca^{2+}$ substitution in the structure of ettringite or AFm phases, as previously postulated in the literature. Sorption of Zn^{2+} onto C–(A)–S–H could also occur, but could not explain by itself the good retention of zinc.

Acknowledgements

The authors are deeply grateful to N. Rafai (LERM, France) for characterization of the leached samples by SEM/EDX, and to J. Bourthoumieux for synthesis of Zn-substituted AF_t and AF_m phases.

References

[1] L. Cecille, C. Kertesz (Eds.), Treatment and Conditioning of Radioactive Incinerator Ashes, Elsevier Science Publishers Ltd, London, 1991, p. 239.
[2] G. Arliguie, J. Grandet, Etude par calorimétrie de l'hydratation du ciment Portland en présence de zinc, Cem. Concr. Res. 15 (1985) 825–832.
[3] G. Arliguie, J. Grandet, Study of cement hydration in presence of zinc—influence of gypsum content, Cem. Concr. Res. 20 (1990) 346–354.
[4] J. Dale Ortego, S. Jackson, G.S. Yu, H. McWhinney, D.L. Cocke, Solidification of hazardous substances—a TGA and FTIR study of Portland cement containing metal nitrates, J. Environ. Sci. Health A24 (1989) 589–602.
[5] M.J. Cullinane Jr., R.M. Bricka, N.R. Francingues Jr., An assessment of materials that interfere with stabilization/solidification processes, Report EPA/600/9-87/015, Environmental Protection Agency, WA, 1987, pp. 64–71.
[6] I. Fernandez Olmo, E. Chacon, A. Irabien, Influence of lead, zinc, iron(III) and chromium(III) oxides on the setting time and strength development of Portland cement, Cem. Concr. Res. 31 (2001) 1213–1219.
[7] I.W. Hamilton, N.M. Sammes, Encapsulation of steel foundry dusts in cement mortar, Cem. Concr. Res. 29 (1999) 55–61.
[8] P.A. Spear, Zinc in Aquatic Environment: Chemistry, Distribution and Toxicology, National Research Council of Canada, Environmental Secretariat Publication 17589, Publications NRCC/CNRC, Ottawa, 1981.
[9] Toxicity summary for zinc and zinc compounds, in: Risk Assessment Information System, University of Tennessee, 2009, http://rais.ornl.gov.
[10] R.A. Goyer, Toxic effect of metals, in: M.O. Amdur, J. Doull, C.D. Klassen (Eds.), Casarett and Doull's Toxicology, The Basic Science of Poisons, Permagon Press, New York, 1991, p. 1032.
[11] S. Berger, C. Cau Dit Coumes, P. Le Bescop, D. Damidot, Hydration of calcium sulfoaluminate cement by a $ZnCl_2$ solution: investigation at early age, Cem. Concr. Res. 30 (2009) 1180–1187.
[12] S. Berger, C. Cau Dit Coumes, P. Le Bescop, D. Damidot, Stabilization of $ZnCl_2$-containing wastes using calcium sulfoaluminate cement: cement hydration,

strength development and volume stability, J. Hazard. Mater., this issue, doi:10.1016/j.jhazmat.2011.07.095.
[13] F. Adenot, M. Buil, Modeling of the corrosion of cement paste by deionized water, Cem. Concr. Res. 22 (1992) 489–495.
[14] S. Peysson, J. Pera, M. Chabannet, Immobilization of heavy metals by calcium sulfoaluminate cement, Cem. Concr. Res. 35 (2005) 2261–2270.
[15] S. Berger, C. Cau Dit Coumes, P. Le Bescop, D. Damidot, Influence of a thermal cycle at early age on the hydration of calcium sulphoaluminate cements with variable gypsum contents, Cem. Concr. Res. 41 (2011) 149–160.
[16] J.T. Kloprogge, L. Hickey, R.L. Frost, The effects of synthesis pH and hydrothermal treatment on the formation of zinc aluminum hydrotalcites, J. Solid State Chem. 177 (2004) 4047–4057.
[17] S. Miyata, The synthesis of hydrotalcite-like compounds and their structures and physico-chemical properties – I: the systems Mg^{2+}–Al^{3+}–NO_3^-, Mg^{2+}–Al^{3+}–Cl^-, Mg^{2+}–Al^{3+}–ClO_4^-, Ni^{2+}–Al^{3+}–Cl^-, and Zn^{2+}–Al^{3+}–Cl^-, Clays Clay. Miner. 23 (1975) 369–375.
[18] T. Ishikawa, K. Matsumoto, K. Kandori, T. Nakayama, Anion-exchange and thermal change of layered zinc hydroxides formed in the presence of Al(III), Colloids Surf. A: Physicochem. Eng. Asp. 293 (2007) 135–145.
[19] H. Pollemann, A. Vogel, JCPDS file number 44-066, Friedrich-Alexander Univ., Erlangen-Nurnberg, Erlangen, Germany, ICDD Grant-in-Aid, 1993.
[20] V. Albino, R. Cioffi, M. Marroccoli, L. Santoro, Potential application of ettringite generating systems for hazardous waste stabilization, J. Hazard. Mater. 51 (1996) 241–252.
[21] R. Berardi, R. Cioffi, L. Santoro, Matrix stability and leaching behaviour in ettringite-based stabilization systems doped with heavy metals, Waste Manage. 17 (1997) 535–540.
[22] J. Pera, J. Ambroise, M. Chabannet, Valorization of automotive shredder residue in building materials, Cem. Concr. Res. 34 (2004) 557–562.
[23] M.L.D. Gougar, B.E. Scheetz, D.M. Roy, Ettringite and C–S–H Portland cement phases for waste immobilization: a review, Waste Manage. 16 (1996) 295–303.
[24] G.J. Mc Carthy, D.J. Hassett, J.A. Bender, Synthesis, crystal chemistry and stability of ettringite, a material with potential applications in hazardous waste immobilization, Mat. Res. Soc. Symp. Proc. 245 (1992) 129–140.
[25] S. Auer, H.J. Kuzel, H. Pollmann, F. Sorrentino, Investigation on MSW fly ash treatment by reactive calcium aluminates and phases formed, Cem. Concr. Res. 25 (1995) 1347–1359.
[26] H.F.W. Taylor, Cement Chemistry, 2nd edition, Thomas Telford, 1997, p. 169.
[27] I. Odler, S. Abdul-Maula, Possibilities of quantitative determination of the AFt-(ettringite) and AFm- (monosulphate) phases in hydrated cement pastes, Cem. Concr. Res. 14 (1984) 133–141.
[28] E.T. Carlson, H.A. Berman, Some observations on the calcium aluminate carbonate hydrates, J. Res. Natl. Bur. Stand. 64A (1960) 333–341.
[29] G. Arliguie, J.P. Ollivier, J. Grandet, Etude de l'effet retardateur du zinc sur l'hydratation de la pâte de ciment Portland, Cem. Concr. Res. 12 (1982) 79–86.
[30] G. Arliguie, J. Grandet, Influence de la composition d'un ciment Portland sur son hydratation en présence de zinc, Cem. Concr. Res. 20 (1990) 517–524.
[31] J. Dale Ortego, Y. Barroeta, F.K. Cartledge, H. Akhter, Leaching effects on silicate polymerization—an FTIR and ^{29}Si NMR study of lead and zinc in Portland cement, Environ. Sci. Technol. 25 (1991) 1171–1174.
[32] M. Yousuf, A. Mollah, K. Vempati, T.C. Lin, D.L. Cocke, The interfacial chemistry of solidification/stabilization of metals in cement and pozzolanic materials systems, Waste Manage. 15 (1995) 137–148.
[33] S. Asavapisit, G. Fowler, C.R. Cheeseman, Solution chemistry during cement hydration in the presence of metal hydroxide wastes, Cem. Concr. Res. 27 (1997) 1249–1260.
[34] T. Ishikawa, K. Matsumoto, A. Yasukawa, K. Kandori, T. Nakayama, T. Tsubota, Influence of metal ions on the formation of artificial zinc rusts, Corros. Sci. 46 (2004) 329–342.
[35] I. Joy Bear, I.E. Grey, I.E. Newnham, L.J. Rogers, The $ZnSO_4{\cdot}3Zn(OH)_2$–H_2O system. I. Phase formation, Aust. J. Chem. 40 (1987) 539–569.
[36] C. Forano, T. Hibino, F. Leroux, C. Taviot Gueho, Layered double hydroxides, in: F. Bergaya, B.K.G. Theng, G. Lagaly (Eds.), Handbook of Clay Science, Chapter 13.1, Developments in Clay Science, vol. 1, Elsevier, 2006, pp. 1021–1095.
[37] O.K. Srivastava, E.A. Secco, Studies on metal hydroxy compounds. I. Thermal analyses of zinc derivatives ε-$Zn(OH)_2$, $Zn_5(OH)_8Cl_2{\cdot}H_2O$, β-ZnOHCl and ZnOHF, Can. J. Chem. 45 (1967) 579–583.
[38] F. Ziegler, R. Giere, C.A. Johnson, Sorption mechanisms of zinc to calcium silicate hydrate: sorption and microscopic investigations, Environ. Sci. Technol. 35 (2001) 4556–4561.
[39] I. Moulin, W.E.E. Stone, J. Sanz, J.Y. Bottero, F. Mosnier, C. Haehnel, Lead and zinc retention during hydration of tri-calcium silicate, a study by sorption isotherms and ^{29}Si NMR spectroscopy, Langmuir 15 (1999) 2829–2835.
[40] F. Ziegler, A.M. Sheidegger, C.A. Johnson, R. Dähn, E. Wieland, Sorption mechanisms of zinc to calcium silicate hydrate: X-ray absorption fine structure (XAFS) investigation, Environ. Sci. Technol. 35 (2001) 1550–1555.
[41] S. Komarneni, E. Breval, D.M. Roy, R. Roy, Reactions of some calcium silicates with metal cations, Cem. Concr. Res. 18 (1988) 204–220.
[42] A. Stumm, K. Garbev, G. Beuchle, L. Black, P. Stemmermann, R. Nüesch, Incorporation of zinc into calcium silicate hydrates – Part I – Formation of C–S–H (I) with C/S = 2/3 and its isochemical counterpart gyrolite, Cem. Concr. Res. 35 (2005) 1665–1675.
[43] A.K. Karamalidis, D.A. Dzombak, Surface Complexation Modelling: Gibbsite, John Wiley and Sons, Hoboken, New Jersey, 2010, p. 294.
[44] O.S. Pokrovsky, J. Viers, R. Freydier, Zinc stable isotope fractionation during its adsorption on oxides and hydroxides, J. Colloid Interface Sci. 291 (2005) 192–200.
[45] G. Micera, C. Gessa, P. Melis, A. Premoli, R. Dallochio, S. Deiana, Zinc(II) adsorption on aluminum hydroxide, Colloids Surf. 17 (1986) 389–394.
[46] T.P. Trainor, G.E. Brown Jr., G.A. Parks, Adsorption and precipitation of aqueous Zn(II) on alumina powders, J. Colloid Interface Sci. 231 (2000) 359–372.
[47] D.R. Roberts, R.G. Ford, D.L. Sparks, Kinetics and mechanisms of Zn complexation on metal oxides using EXAFS spectroscopy, J. Colloid Interface Sci. 263 (2003) 364–376.